

# Pricing Barrier Options with DeepBSDEs<sup>\*†</sup>

Narayan Ganesan<sup>1</sup>, Yajie Yu<sup>1</sup>, and Bernhard Hientzsch<sup>1</sup>

<sup>1</sup>Corporate Model Risk, Wells Fargo (as of March 2022)

## Abstract

This paper presents a novel and direct approach to solve boundary and final-value problems, corresponding to barrier options, using forward pathwise deep learning and forward-backward stochastic differential equations (FBSDEs). Barrier instruments are instruments that expire or transform into another instrument if a barrier condition is satisfied before maturity; otherwise they perform like the instrument without the barrier condition. In a PDE formulation, this corresponds to adding boundary conditions to the final value problem. The deep BSDE methods developed so far have not addressed barrier/boundary conditions directly. We extend the pathwise forward deep BSDE to the barrier condition case by adding nodes to the computational graph to explicitly monitor the barrier conditions for each realization of the dynamics as well as nodes that preserve the time, state variables, and trading strategy value at barrier breach or at maturity otherwise. Given these additional nodes in the computational graph, the forward loss function quantifies the replication of the barrier or final payoff according to a chosen risk measure such as squared sum of differences. The proposed method can handle any barrier condition in the FBSDE set-up and any Dirichlet boundary conditions in the PDE set-up, both in low and high dimensions.

## 1 Introduction

Deep Learning and Deep Neural Networks have been applied to numerically solve high-dimensional nonlinear PDEs via the use of Forward-Backward Stochastic Differential Equations or FBSDEs (see (Han et al., 2018)). In particular, (Han et al., 2018) applied it to a quantitative finance pricing problem to price a combination of two Call options under differential rates (different lending and borrowing interest rates), a nonlinear problem that was also studied in (Mercurio, 2015). In related work, (Chan-Wai-Nam et al., 2019) and (Raissi, 2018) also showed the applicability of deep learning in solving FBSDEs. The overview paper of DeepBSDE methods (Hientzsch, 2019) introduces how FBSDE and certain deep learning methods can be used to solve quantitative finance problems.

This paper presents a novel approach to solve boundary and final value problems (corresponding to barrier options) with pathwise forward deep learning approaches (“forward DeepBSDE”). The approach

---

<sup>\*</sup>Self-archived author accepted manuscript version of the article published in Journal of Computational Finance, Volume 25, Number 4, Pages 1-25, DOI: <https://doi.org/10.21314/JCF.2021.016>

<sup>†</sup>Any opinions, findings, conclusions, and/or recommendations expressed in this material are those of the authors and do not necessarily reflect the views of any past, current, or future employers (such as Wells Fargo Bank, N.A., its parent company, affiliates, and subsidiaries) of any of the authors.

adds nodes to the computational graph to explicitly monitor the barrier conditions for each realization of the dynamics. In case of barrier breach, the nodes record the time and underlying state variables; otherwise they record the final time and value at maturity which is used to determine the final payoff. The forward loss function then quantifies the replication of the barrier or final payoff according to a chosen risk measure such as squared sum of differences.

The simplest forms of barrier options are single-underlier or basket knock-in or knock-out options in which the barrier condition only involves the current value of the underlier or the basket and compares it to a given barrier level, which is often a given constant. Let  $S_t$  be that underlier or the value of the basket. Examples shown in Table 1 include the variants of simple barrier Calls in this setting, for strike price ( $K$ ), time to maturity ( $T$ ), a barrier positions  $U_t$  and  $L_t$  (possibly time dependent) and the vanilla Call price  $V(S_t, K, T - t)$ . Put versions of these examples are obtained by replacing Calls and Call prices by Puts and Put prices everywhere.

Name	Barrier Condition	Knocked-in Instrument	In-Rebate	Knocked-In Instrument Value	Final Payoff if not Breached
Up-and-Out Call	$S_t \geq U_t$ (Upper Barrier Position)	$G_t$		0	$\max(S_T - K, 0)$
Down-and-Out Call	$S_t \leq L_t$ (Lower Barrier Position)	$G_t$		0	$\max(S_T - K, 0)$
Up-and-In Call	$S_t \geq U_t$ (Upper Barrier Position)	0		$V(S_t, K, T - t)$	0
Down-and-In Call	$S_t \leq L_t$ (Lower Barrier Position)	0		$V(S_t, K, T - t)$	0

Table 1: Summary of basic barrier Call instruments

The simplest barrier options are those with barrier at some constant level which is active for the entire life of the instrument. Two standard examples: A standard Up-and-Out Call option with upper barrier  $B$  will pay the final Call payoff unless the underlier  $S$  of the option was observed at a level  $S \geq B$  during the life of the option in which case it will pay a rebate  $G$ . A standard Up-and-In Call option with upper barrier  $B$  will pay the final Call payoff only if the underlier  $S$  of the option was observed at a level  $S \geq B$  during the life of the option and otherwise will pay a rebate  $G$ .

Given a knock-in instrument, a model, and a valuation approach applied to that model, the knocked-in instrument at barrier breach can be replaced by an immediate payment of the value of the knocked-in instrument according to the model without impacting the value of the knock-in instrument before barrier breach. In this way, one can restrict oneself to the case of knock-out instruments with rebates.

There are many instruments with barrier features in Quantitative Finance. There are also many other applications in natural sciences, engineering, and economics that involve bounded domains and boundaries in stochastic analysis and stochastic processes. Similarly, PDE models in natural sciences and engineering are often posed in bounded domains with boundary conditions imposed at the boundary. The extensions presented in this paper to the forward DeepBSDE method allow this new methodology to be applied to all these situations and applications.

The rest of the paper is organized as follows: Section 2 presents a brief overview of Forward-Backward Stochastic Differential Equations as applied to options pricing. Section 3 discusses the

technique behind DeepBSDE approach to solving traditional option pricing problem and a description of the approach to problems with barriers. Section 4 discusses other approaches that are currently used or proposed for pricing barrier options and outlines their limitations. Section 5 describes our approach, which employs barrier tracking variables as a part of the DeepBSDE graph. Section 6 presents the results of pricing barrier options in one and ten dimensions using this approach. The paper concludes with some remarks.

## 2 Problem Setup and Forward-Backward SDEs

For a general introduction to FBSDE and their relations to nonlinear parabolic PDE and/or quantitative finance, see (El Karoui et al., 1997) and (Perkowski, 2010). (Han et al., 2018) presented the first application of DeepBSDE method to the pricing of European options under differential rates. (Hientzsch, 2019) provides an overview of the types of problems in quantitative finance that can be solved using DeepBSDE and FBSDE. In this paper, we will discuss only specific aspects of PDEs and FBSDEs relevant to our setting.

We will first discuss how a semilinear parabolic PDE can give rise to a FBSDE. A semilinear parabolic PDE is a PDE of the form:

$$\begin{aligned} \frac{\partial u}{\partial t}(t, x) + Lu(t, x) + f(t, x, u(t, x), a^T(t, x)\nabla_x u(t, x)) &= 0 \\ Lu(t, x) &:= \frac{1}{2}\mathbf{Tr}(a(t, x)a^T(t, x)\nabla_x^2 u(t, x)) + \nabla_x u(t, x)b(t, x) \end{aligned} \quad (1)$$

defined on a domain  $D \subset \mathbb{R}^d$  and  $x \in D$ . In quantitative finance and other applications, these PDE are often posed with terminal conditions,  $u(T, x) = g(T, x)$  for a given function  $g$ .

Consider an Itô process  $X$  given by:

$$dX_t = b(t, X_t)dt + a(t, X_t)dW_t \quad (2)$$

where  $X_t \in \mathbb{R}^d$ ,  $dW_t \in \mathbb{R}^d$ ,  $b(t, X) \in \mathbb{R}^d$  and  $a(t, X) \in \mathbb{R}^{d \times d}$ , with uncorrelated  $dW_t$  and correlations expressed through  $a(t, X)$ , defined on an appropriate filtration  $\mathcal{F}_t$ . For every  $(t, x)$  we will consider a version of  $X$  that starts (or arrives) at time  $t$  in  $x$  and call it  $X^{t,x}$ . Let  $Y_t$  be  $u(t, X_t)$ . Then  $Y_t$  satisfies the Backward Stochastic Differential Equation

$$dY_t = -f(t, X_t, Y_t, a^T(t, X_t)\nabla u(t, X_t))dt + (\nabla u(t, X_t))^T a(t, X_t)dW_t \quad (3)$$

along with the equation for  $X_t$ , satisfying (2). A terminal condition  $u(T, x) = g(T, x)$  for the PDE translates into a terminal condition for the BSDE  $Y_T = g(T, X_T)$ .

With  $\pi_t = \nabla_x u(t, X_t)$ , the BSDE (3) can be written

$$-dY_t = f(t, X_t, Y_t, a^T(t, X_t)\pi_t)dt - \pi_t^T a(t, X_t)dW_t \quad (4)$$

Equations (2) and (4) together describe the dynamics of solution  $u(t, x)$  of PDE (1) within the framework of FBSDE. Similarly, one can prove there are functions  $u$  and  $\pi$  such that  $Y_s^{t,x} = u(s, X_s^{t,x})$  and  $\pi_s^{t,x} = \pi(s, X_s^{t,x})$ , that  $\pi(t, x) = \nabla_x u(t, x)$ , and that  $u$  then solves the PDE (1) in the appropriate sense, see (El Karoui et al., 1997) and (Perkowski, 2010).

So, instead of solving a PDE (1) for  $u$ , we can solve the FBSDE (4) by finding stochastic processes  $Y_t$  and  $\pi_t$ . Instead of finding a process  $\pi_t$  we can also try to find a function  $\pi(t, x)$  (or different functions for different  $t$ ) such that  $\pi_t = \pi(t, X_t)$ , as inspired by the expression for  $\pi_t$  given above.

Notice that however the FBSDE formulation as written in (2) and (4) is more general than the original PDE. For instance, the terminal condition can be a random variable  $G_T$  measurable as of  $\mathcal{F}_T$ , depending on the paths of  $X_t$  and  $W_t$ , rather than a function of just the final value  $X_T$ . Then, solution functions  $u$  and portfolio functions  $\pi$  would potentially also have more general forms and more arguments and might also depend on the state of additional processes that capture the path-dependency of the terminal condition and allow the replication or risk management of the same. There is no straightforward way to give equivalent PDE formulations at this level of generality, in fact there might not exist a straightforward one.

The above relation between PDE and FBSDE can be illustrated explicitly, for instance in the case of risk-neutral valuation of simple derivatives which obey the Black-Scholes-Merton equation

$$\frac{\partial u}{\partial t} + r(t, x)x \frac{\partial u}{\partial x} + \frac{\sigma^2(t, x)}{2} x^2 \frac{\partial^2 u}{\partial x^2} - r(t, x)u(t, x) = 0 \quad (5)$$

with the underlying  $X$ , driven by an Itô process, in the risk-neutral measure (Shreve, 2004), under which  $X$  follows

$$dX = r(t, x)X dt + \sigma(t, x)X dW_t, \quad (6)$$

where  $r(t, x)$  is the risk-free rate and  $\sigma(t, x)$  is the volatility of the underlier. Under this setup, for any function  $y(t, x)$ , by Itô process rule,

$$dy(t, x) = \left( \frac{\partial y}{\partial t} + r(t, x)x \frac{\partial y}{\partial x} + \frac{\sigma(t, x)^2}{2} x^2 \frac{\partial^2 y}{\partial x^2} \right) dt + \sigma(t, x)x \frac{\partial y}{\partial x} dW_t \quad (7)$$

If  $y(t, x)$  is to describe the behavior of the value of the derivative  $u(t, x)$ , it has to obey equation (5), along with the terminal condition,  $y_T = g(T, X_T)$ . Under this assumption (5), the first term on right side in the parenthesis of equation(7) must obey,

$$\frac{\partial y}{\partial t} + r(t, x)x \frac{\partial y}{\partial x} + \frac{\sigma(t, x)^2}{2} x^2 \frac{\partial^2 y}{\partial x^2} = r(t, x)y \quad (8)$$

substituting for the term above in equation(7), leads to the update equation for  $y(t, x)$ :

$$dy(t, x) = r(t, x)y(t, x)dt + \sigma(t, x)x \frac{\partial y}{\partial x} dW_t \quad (9)$$

Now denoting  $Y_t = y(t, X_t)$ ,  $\pi(t) = \frac{\partial y}{\partial x}(t, X_t)$ ,  $a(t, X_t) = \sigma(t, X_t)X_t$ , and  $f(t, X_t, Y_t, Z_t) = -r(t, X_t)Y_t$ , this update equation corresponds to (4).

Here we are interested in the extension to PDE boundary conditions corresponding to barrier options. For PDEs, Dirichlet boundary conditions are imposed in addition to the PDE (1):

$$u(t, x) = g_B(t, x) \text{ for } (t, x) \in B \quad (10)$$

corresponding to standard barrier conditions with barrier domain  $B$ . Final value conditions can be included so that  $g_B(T, x) = g(T, x)$  with the previously defined  $g$ . We assume that this is done.

The function  $g_B$  will encode the specific barrier option treated. For a knock-out barrier Call option, the barrier and final payoff is given by

$$g_B(t, X_t) = \begin{cases} \max(X_t - K, 0.0) & \text{if } t = T \\ 0.0 & \text{if } t \leq T \end{cases} \quad (11)$$

A knock-in barrier Call option would be given by

$$g_B(t, X_t) = \begin{cases} 0.0 & \text{if } t = T \\ V(X_t, K, T - t) & \text{if } t \leq T \end{cases} \quad (12)$$

with  $V(X_t, K, T - t)$  the vanilla Call price. For both examples, we assume that the barrier is not active at  $T$ . Note that  $g_B$  is the same regardless of the level or number of barriers. The first covers Up-and-Out, Down-and-Out, and Double-Barrier-out Calls and similarly the second covers Up-and-In, Down-and-In, and Double-Barrier-in Calls.

To include barrier conditions in the FBSDE formulation corresponding to the PDE, the process  $Y_t$  that we are trying to determine will follow the FBSDE (2) and (4) when  $X_t$  is outside of  $B$  while the value of the process  $Y_t$  is directly given by  $g_B(t, X_t)$  inside of  $B$  (where maturity is included in  $B$ ).

More generally, define the barrier condition  $C_t$  (eg: the barrier breach) as a random variable with values **true** and **false** which is measurable (computable) given the information about the dynamics  $X_s, (s \leq t)$ . If a barrier domain  $B$  in terms of state  $(t, X_t)$  is given, then  $C_t = (t, X_t) \in B$ . Similarly, define  $\tau$  as the first time  $(t, X_t)$  is within  $B$  respectively  $C_t$  is true. The value of  $Y_t$  at  $\tau$  can be given as a random variable  $G_\tau$  which is measurable (computable) given  $X_s, (s \leq \tau)$ . If  $g_B$  is given as above,  $G_\tau = g_B(\tau, X_\tau)$ .

Now a FBSDE with barrier condition can be formulated as a FBSDE with random terminal time  $\tau$ . Given a stopping time  $\tau$ , for  $t < \tau$ ,  $Y_t$  follows (4):

$$-dY_t = f(t, X_t, Y_t, a^T(t, X_t)\pi_t)dt - \pi_t^T a(t, X_t)dW_t$$

For times  $t \geq \tau$ , we assume the FBSDE is stopped

$$Y_t = G_\tau \quad (13)$$

or in the barrier domain case,

$$Y_t = g_B(\tau, X_\tau). \quad (14)$$

For completeness, we set  $\pi_t = 0$  for  $t \geq \tau$ .

For general barrier conditions  $C_t$ , the stopping time is defined as

$$\tau = \inf \{t \in [0, T] : C_t \text{ is true}\} \wedge T \quad (15)$$

while for the barrier domain case, it is

$$\tau = \inf \{t \in [0, T] : (t, X_t) \in B\} \wedge T \quad (16)$$

Just as before, the stopped FBSDE formulation given here is much more general than the PDE formulation presented earlier. For instance, the barrier trigger and also the value of the option once

barrier is triggered could be given in terms of time averages, lookbacks to maximum or minimum, realized variance, etc. Here, we will consider the barrier domain / boundary value setting.

For this setting, Lejay (2002) treats the case where either boundary values are zero or they are given by the values of a bounded and Hölder continuous function  $\phi(t, x)$  that is defined everywhere and agrees with the boundary values and final values in the appropriate domain. For the PDE, he considers the weak solution defined through a variational form where the boundary condition is treated as an essential condition (test and trial spaces are  $H_0^1$  on the complement of  $B$  respectively the appropriate extension to nonzero boundary values). He then proves that weak solutions of the PDE in that sense can be identified with solutions of the stopped FBSDE. In this setting and under appropriate conditions, boundary conditions would be assumed pointwise. In a different context, Kremsner et al. (2020) explores the relation between elliptical PDE with Dirichlet boundary conditions and stopped FBSDE (corresponding to a setting where neither generator nor coefficients depend on time). These Dirichlet boundary conditions are given by the values at the boundary of a continuous bounded function  $g$  defined on the domain of interest. Kremsner et al. (2020) shows that a classic solution of the PDE can be used to construct a solution of the FBSDE and cites Pardoux (1998) which shows that given a solution of the FBSDE, one obtains a continuous viscosity solution of the elliptical PDE, and boundary conditions would be assumed pointwise. In both cases settings, if the solution is smooth enough, the weak respectively viscosity solution will also be a classical solution. Thus, under these conditions, one can use FBSDE to find solutions of the PDE that will assume the boundary conditions pointwise. We will not further consider the theory for boundary value problems or stopped FBSDE for more general cases or under weaker conditions in this paper.

In the risk-neutral case as mentioned above, if the barrier option is given by a barrier domain  $B$  and a barrier function  $g_B(t, x)$ , one can characterize the solution of the boundary value problem as

$$u(t, x) = E[g_B(\tau_T^{t,x}, X_{\tau_T^{t,x}}^{t,x})e^{-\int_t^{\tau_T^{t,x}} r(s, X_s^{t,x})ds}] \quad (17)$$

where the expectation is taken with respect to the risk-neutral measure (Shreve, 2004) and the stopping time is here defined as

$$\tau_T^{t,x} = \inf \{s \in [0, T] : (s, X_s^{t,x}) \in B\} \wedge T \quad (18)$$

using the version  $X_s^{t,x}$  of  $X$  started in  $x$  at time  $t$ .

For any general FBSDE problem as in Equations (2) and (4), applying a simple Euler-Maruyama discretization for both  $X_t$  and  $Y_t$ , we obtain

$$X_{t_{i+1}} = X_{t_i} + b(t_i, X_{t_i})\Delta t_i + a(t_i, X_{t_i})\Delta W^i \quad (19)$$

$$Y_{t_{i+1}} = Y_{t_i} - f(t_i, X_{t_i}, Y_{t_i}, \pi_{t_i})\Delta t_i + \pi_{t_i}^T a(t_i, X_{t_i})\Delta W^i \quad (20)$$

This can be used to time-step both  $X_t$  and  $Y_t$  forward.

$X_t$  will be simulated forward in a pathwise sense. The equation for  $Y$  can be time-stepped forward in a pathwise sense or can be understood as an equation that connects a value function for  $Y$  at time  $t_i$  with a value function of  $Y$  at time  $t_{i+1}$ , either in an exact or a least square sense (assuming that the  $\pi_{t_i}$  is given as a function or process). Under appropriate conditions, one can solve the  $Y$  equation for  $Y_{t_i}$  in terms of  $Y_{t_{i+1}}$  and then time-step it also backward. A value function can be fitted to pathwise

values either as a post-processing step or as an additional term in the appropriate loss function. In the methods considered in this paper, we will time-step the  $Y$  equation pathwise forward (forward pathwise FBSDE methods).

### 3 Solving BSDE with Deep Neural Networks

We will first discuss application to European option pricing (see (Han et al., 2018)). The FBSDE is first discretized in time as in (19) and (20). The portfolio process  $\pi_t$  is represented by functions  $p_n(X_{t_n}) = \pi(t_n, X_{t_n})$ , one for each time  $t_n$ , and each function  $p_n(X_{t_n})$  is given as a deep neural network. The initial value of the portfolio at the fixed  $X_0$  and the initial portfolio composition  $p_0$  are given as constants.

To generate a realization/training sample, one first generates a realization of  $X_{t_n}$  by (19) and then given the current parameter values for  $Y_0$  and all the  $\pi_{t_n} = p_n$  networks, one computes  $Y_{t_n}$  pathwise and finally  $Y_T = Y_{t_N}$  step by step by (20). The  $L^2$  norm of the replication error  $Y_{t_N} - g(t_N, X_{t_N})$  is used as a loss function.

Instead of using a constant  $X_0$ , one can start with a randomly generated  $X_0$ . Under those circumstances, one determines the parameters of the network representing the function  $Y_0(X_0)$  rather than a single value  $Y_0$  (and also a  $\pi_0 = p_0$  network and its parameters). We have also implemented that method. (Han et al., 2018) mention the forward approach for random  $X_0$  as a possibility on page 8509 but we are not aware of any implementation of this method besides our own to the best of our knowledge. One can also use other risk measures defined from the replication error in the optimization. Finally, the loss function is optimized with stochastic optimization methods such as mini-batch stochastic gradient descent combined with Adam optimizers or other appropriate deep learning methods to determine the parameters of the  $p_n$  and  $Y_0$  network.

Figure 1 shows the computational graph for the forward method for European options with random  $X_0$ .

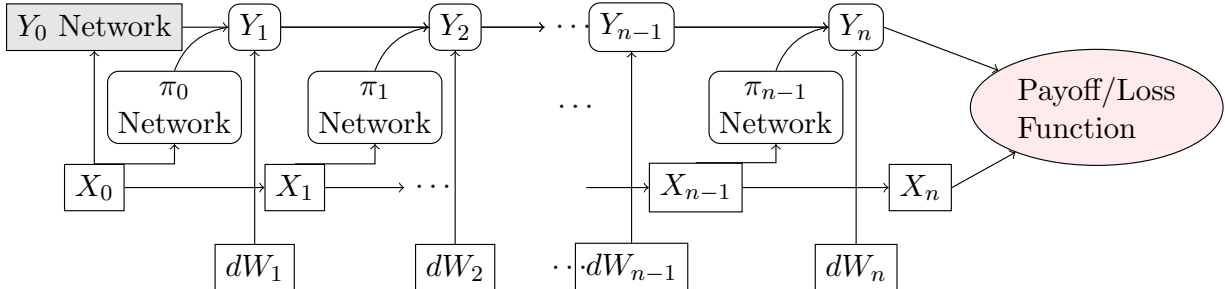


Figure 1: Computational graph for forward DeepBSDE

As seen earlier, in the time-continuous case,  $\pi_t = \nabla_x u(t, X_t)$ , which in financial terms corresponds to delta-hedging according to some value function  $u$ . In the case the FBSDE, time-continuous or not, is expressed as minimization, the  $\pi_t$  determined during the optimization does not necessarily have to be equal to  $\nabla_x u(t, X_t)$  although it often approximates it to a certain extent. In the time-discrete case, the analytical solution is no longer guaranteed to minimize the replication error, but reflects a good

benchmark and what one would achieve by continuous delta-hedging with that value function. Later, we will compare the hedging/replication strategy given by the optimized DNN with the one implied by the analytical solution, for the barrier case.

We now present the fundamental idea for the barrier case and will leave the implementation details to a later section. The fundamental idea to extend the forward pathwise method to the barrier case is that the barrier breach time and place (together with maturity) takes the place of maturity as the first time and place at which the value of  $Y_t$  is known and any approximation of  $Y$  should try to approximate that first known value well regardless whether it was specified in the problem as a final value or a barrier condition value.

The first time at which the dynamics  $X_t$  enters the barrier domain  $B$  or satisfies the barrier condition  $C_t$  is called barrier touch/breach time and is denoted  $\tau_T^{t,x}$  as introduced above (where maturity and final values are included in the domain  $B$  and the  $g_B$ ).

Thus, the loss function to be minimized, according to some norm/risk measure (for instance,  $L^2$  norm), is

$$Y_{\tau_T^{t,x}} - g_B \left( \tau_T^{t,x}, X_{\tau_T^{t,x}} \right) \quad (21)$$

If one would try to learn functions for  $Y$  at each time going forward rather than work with pathwise values, this would couple all functions and values at all time steps together across all paths and all of them would be trained from the replication mismatch at maturity or barrier breach, leading to a more complex, harder, and harder to train problem. Also, if one determines solution functions, one needs a way to enforce the barrier values in the regions where the dynamics enters the barriers, and an efficient operational global characterization of the barrier domains. For backward pathwise or function based methods, one would need alternative formulations, not the stopped characterization, which only works forward in time until the barrier has been first breached. We leave adaptations of such methods to the barrier case to future publications and present here the forward pathwise method which does not have such issues and is more straightforward.

## 4 Other Approaches to Pricing Barrier Options

We briefly review some of the techniques used in practice to price such barrier options.

**PDE Based Approaches:** Options pricing via the solution of PDE with finite differences or finite elements or other standard approaches in high dimensions (many underlying assets) poses difficulties due to extreme storage and computational requirements to compute and store the values on a grid that covers the domain. Accuracy and stability requirements often require larger grids than what is achievable with given resources. In traditional PDE schemes, the PDE grid is generated with sufficiently small spacing for finite difference methods in region of interest that includes final time  $T$  and barrier positions. The finite difference time-stepping proceeds from the final time  $T$  along the time axis spanning a domain bounded on one or both sides by barriers and/or other appropriate boundary conditions. The time-stepping scheme is then applied to determine the values at grid points going backward in time. PDE techniques are well studied and applied widely, however their applicability is limited and is best suited to pricing derivatives on fewer number of underliers due to issues with storage and computational requirements caused by dimensionality. However, PDE techniques can model at least some nonlinear pricing.



**Monte-Carlo Based Approaches:** Barrier options in high dimensions are often priced by Monte-Carlo approaches. This includes generating multiple independent sample paths of the underliers in order to compute the realized payoff at maturity or barrier breach along each path and discounting it to the present time and averaging the payoffs to determine the value of the option. While generating sample paths in high dimensions certainly increases in difficulty and resource requirements with the dimension, these requirements do not depend exponentially on the number of dimensions as the grid size in PDE. In the case when there are rare events with high impact on the price (such as a knock-out condition on a short or far out barrier for an otherwise high payoff), simulation-based approaches such as Monte-Carlo need to sample those rare events sufficiently well to approximate the price of the instrument well. One of the main limitations of standard Monte-Carlo based approaches is that they can only take into account risk-neutral discounting or other linear pricing approaches and cannot be used to model nonlinear pricing such as the differential rates, in which borrowing and lending attracts different interest rates (Hientzsch, 2019).

**DeepBSDE Based Approaches:** DeepBSDE based approaches as originally proposed in (Han et al., 2018) alleviate the problem of dimensionality by converting the high-dimensional PDEs into Backward Stochastic Differential Equations. The SDEs are then solved as a stochastic optimal control problem by approximating the co-state and initial value of the control problem using Deep Neural Networks. Barrier options require the handling of the barrier boundary conditions as they correspond to ‘knock-in’ and ‘knock-out’s at any time before maturity and such problems are not treated in (Han et al., 2018).

As previously mentioned, the following expression (17) holds in the risk-neutral case:

$$u(t, x) = E[g_B(\tau_T^{t,x}, X_{\tau_T^{t,x}}^{t,x})e^{-\int_t^{\tau_T^{t,x}} r(s, X_s^{t,x})ds}]$$

where the expectation is taken with respect to the risk-neutral measure (Shreve, 2004).

Under this risk-neutral measure  $X$  follows (6) with functions as defined in Section 2,  $\tau_T^{t,x}$  denotes the earlier of barrier breach and maturity, and  $g_B$  combines both final values and barrier values, as defined in Section 3. For knock-out options with zero rebate,  $g_B(t, x)$  will be zero unless  $t = T$ .

Therefore, (17) will in this case simplify to

$$\begin{aligned} u(t, x) &= E[1_{\tau^{t,x} \geq T} g(T, X_T^{t,x}) e^{-\int_t^T r(s, X_s^{t,x}) ds}] \\ &= E[P(\tau^{t,x} \geq T) g(T, X_T^{t,x}) e^{-\int_t^T r(s, X_s^{t,x}) ds}] \end{aligned} \tag{22}$$

This corresponds to an instrument with final payoff

$$P(\tau^{t,x} \geq T) g(T, X_T^{t,x}), \tag{23}$$

which is measurable as of time  $T$  knowing  $X$  up to that time  $T$ . In the case that  $P(\tau^{t,x} \geq T)$  can be written as a (relatively simple and explicit) function of  $X_t = x$  and  $X_T$ , this will give a (different) final value problem for each  $t$  and  $x$ . Informally, the final payoff function is adapted via a Brownian bridge based method to include the probability of breaching the barrier before option maturity.

In recent work, (Yu et al., 2019) have approached the Barrier option pricing as described by the above formula. The computation of probability of breach  $P(\tau^{t,x} \leq T)$  as a function of  $x, t, X_T$ , and

$T$  is analytically tractable for constant barriers and simple risk models (constant drift and volatility of the underlying assets), with the help of results from *Brownian bridge probabilities*. Once  $x$  and  $t$  are fixed, these are standard final value problems that can be solved with the DeepBSDE methods for European options, as demonstrated in (Yu et al., 2019).

A slight generalization can be derived along similar lines for the case in which touching the barrier does not lead to an immediate rebate but only to a changed final payoff, which we denote by  $g_{Br}(T, x)$ . Proceeding similarly to above, one obtains an expectation that can be interpreted as an European option on the final payoff

$$P(\tau^{t,x} \geq T) g(T, X_T^{t,x}) + P(\tau^{t,x} < T) g_{Br}(T, X_T^{t,x}) \quad (24)$$

However, in general, time varying barriers and stochastic risk-models (stochastic interest-rate and volatility of underliers) require Monte-Carlo based approaches to compute the probability. For instance for a single barrier with different levels in multiple time-periods, the probability computation can be extended as follows:

Consider an Up-and-Out barrier option with piecewise constant barriers with  $M$  values within  $0 \leq t \leq T$ , defined by increasing times  $t_0 = 0, t_1, \dots, t_M = T$ :

$$B(t) = \{B_i \text{ for } t_i \leq t < t_{i+1}\} \quad (25)$$

The total probability of no-breach can be computed as product of probabilities of no-breach within each time period, informally written as:

$$\begin{aligned} P(\tau^{t,x} \geq T) &= P_{\text{NoBreach}}(t_0, X(t_0); T, X(T)) \\ &= \prod_{i=0}^{M-1} P_{\text{NoBreach}}(t_i, X(t_i); t_{i+1}, X(t_{i+1})) \end{aligned} \quad (26)$$

where each factor can be computed via Brownian bridge for simple risk-models. However, now one needs to integrate over and/or otherwise sample over the intermediate positions at intermediate times to obtain the barrier probabilities as a function of only initial and final risk factor value. Some other popular varieties of barrier options including multiple barriers (Up and Down barriers), interacting barriers or barrier levels specified as a function of past asset price (maximum drawdown) require more involved Monte-Carlo approaches to compute the probability. Monte-Carlo approaches in higher dimensions to compute these probabilities are computationally expensive and incur higher costs than pricing the option in higher dimensions as outlined above (and therefore will not lead to an efficient method to compute barrier option values through final value problems).

In this work, we propose an original approach using DeepBSDEs that explicitly monitors whether the underliers breach the barrier before maturity and record the state of the barrier option at every time step via nodes in the computational graph, which is then used to determine the appropriate payoff conditions. The technique proposed here is applicable to solving general semi-linear parabolic PDEs or FBSDE in any discipline (in addition to quantitative finance) in which boundary conditions are specified. To the best of our knowledge there is no prior work to handle boundary conditions explicitly in the context of DeepBSDEs, which is important in solving a variety of PDEs and FBSDE with standard and non-standard boundary conditions.

During the publication of this paper, we were made aware of Kremsner et al. (2020), where a similar pathwise forward DeepBSDE approach is used to solve a FBSDE with random terminal time that corresponds to an elliptical boundary value problem and infinite horizon control problems. Unlike them, we handle the parabolic case and our method allows barrier conditions and options that do not correspond to a single barrier domain.

## 5 Deep Neural Network with Barrier Triggers

As mentioned before, we need to keep track of variables that detect whether the barrier was breached (the barrier condition satisfied) and preserve the value of  $X$ ,  $t$ , and  $Y$  at the time of the first barrier breach. In general, we will call these “conditional” variables, or “conditional” tensors (since variables are represented as and called tensors in TensorFlow).

In the time-continuous setting, we need the values of  $\tau_T^{t,x}$ ,  $X_{\tau_T^{t,x}}$ , and  $Y_{\tau_T^{t,x}}$  to compute the loss function (21) or some other risk measure that evaluates how the trading strategy replicates the appropriate payoff. In the time-discrete case, we need to keep track of time-discrete counterparts, which we call **tFP** ( $t$  for payoff), **XFP** ( $X$  for payoff), and **YFP** ( $Y$  for payoff). To write updates for these variables, we need **XTrig** that turns from false (0.0) to true (1.0) once the barrier has been breached. For barrier condition functions  $C_t(t, X_t)$ , this can be defined as

$$\mathbf{XTrig}_i = \begin{cases} \mathbf{XTrig}_{i-1} & \text{if } \mathbf{XTrig}_{i-1} \\ C_{t_i}(t_i, X_{t_i}) & \text{else} \end{cases} . \quad (27)$$

For a problem with a single upper barrier at level  $U$  active during the entire time to maturity, this would read

$$\mathbf{XTrig}_i = \begin{cases} \mathbf{XTrig}_{i-1} & \text{if } \mathbf{XTrig}_{i-1} \\ X_{t_i} \geq U & \text{else} \end{cases} . \quad (28)$$

**XTrig** would be appropriately initialized depending on whether the barrier condition will be checked at time  $t_0$  and could possibly be true there or whether it will only be checked starting at the next time step.

Having defined **XTrig**, we can define **tFP**, **XFP**, and **YFP** as follows:

$$\mathbf{tFP}_i = t_i \times (1.0 - \mathbf{XTrig}_{i-1}) + \mathbf{tFP}_{i-1} \times \mathbf{XTrig}_{i-1} \quad (29)$$

$$\mathbf{XFP}_i = X_{t_i} \times (1.0 - \mathbf{XTrig}_{i-1}) + \mathbf{XFP}_{i-1} \times \mathbf{XTrig}_{i-1} \quad (30)$$

$$\mathbf{YFP}_i = Y_{t_i} \times (1.0 - \mathbf{XTrig}_{i-1}) + \mathbf{YFP}_{i-1} \times \mathbf{XTrig}_{i-1} \quad (31)$$

and initialized with  $\mathbf{tFP}_0 = t_0$ ,  $\mathbf{XFP}_0 = X_{t_0}$ , and  $\mathbf{YFP}_0 = Y_{t_0}$ . These update equations keep copying the underlying  $X$ ,  $Y$ , and  $t$  until the barrier is hit and then stop at the next step, so that the values of the corresponding variables at barrier breach stay in the \*FP versions. If the barrier is never breached, the values of  $t$ ,  $X$ , and  $Y$  at  $t = T = t_N$  will be in  $\mathbf{tFP}_N = t_N$ ,  $\mathbf{XFP}_N = X_{t_N}$ , and  $\mathbf{YFP}_N = Y_{t_N}$ . Thus,  $\mathbf{tFP}_N$ ,  $\mathbf{XFP}_N$ , and  $\mathbf{YFP}_N$  are the appropriate time-discrete analogues of  $\tau_T^{t,x}$ ,  $X_{\tau_T^{t,x}}$ , and  $Y_{\tau_T^{t,x}}$ , and the loss function for the computational graph implementing this time-discrete approach would be

$$\|\mathbf{YFP}_N - g_B(\mathbf{tFP}_N, \mathbf{XFP}_N)\|^2 \quad (32)$$

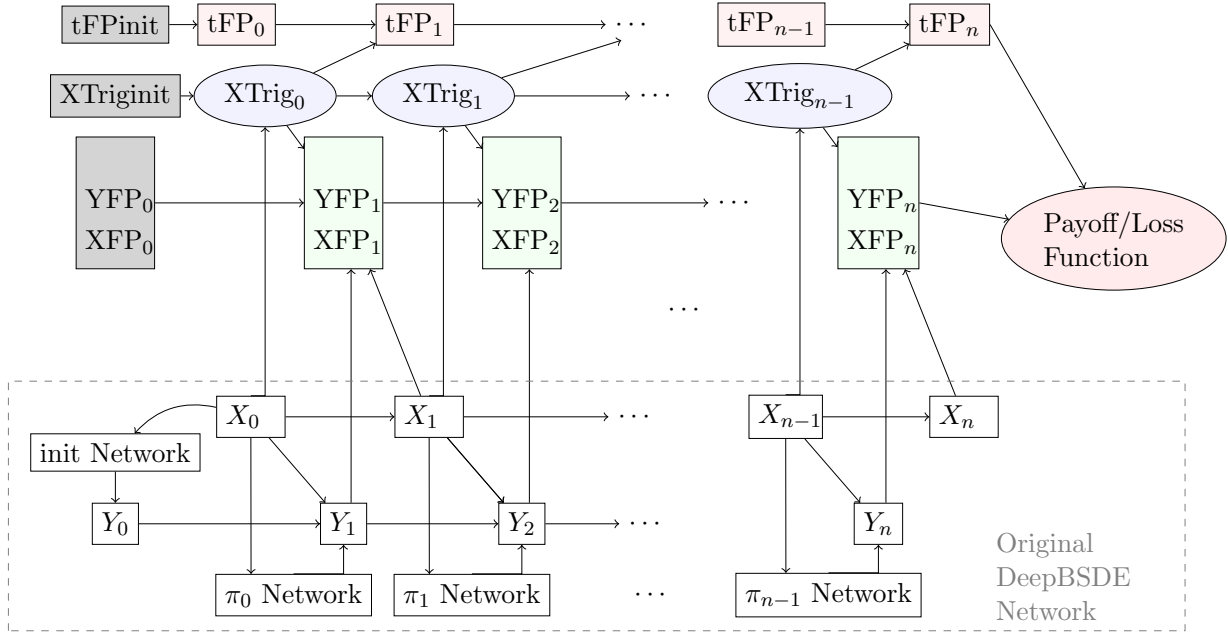


Figure 2: Computational graph for forward DeepBSDE with barrier triggers

or any other appropriate risk measure.

Notice also that time-discretization leads to well-known biases in barrier options. If approximation of a certain time-continuous problem with continuously enforced barriers is desired, there are approaches such as barrier level correction (solving the time-discrete problem with appropriately shifted barrier levels) that will minimize such bias and lead to faster convergence to the solution of the time-continuous problem.

Figure 2 shows the computational graph for the approach just described. The nodes that have been added or changed for the barrier case are shown as color shaded nodes and the nodes from the original forward DeepBSDE computational graph are shown unshaded and enclosed in a dashed box. As discussed above, these additional tensors are needed to preserve the state at barrier breach or maturity and serve to constrain the  $Y_{t_i}$  appropriately so that it follows the FBSDE if not in the barrier domain but approximates the given barrier domain value once it touches the barrier domain.

### 5.1 Behavior of the Conditional Barrier Tensors

Figure 3 shows the values of these barrier breach tracking variables for a case with 500 time steps,  $X_0 = 125$  and an upper barrier at level 150, for the same parameters of the  $X$  dynamics as defined in Table 2, in the next section. The upper panel shows several sample paths of  $X_{t_i}$  while the lower panel shows the corresponding realizations of  $\mathbf{XTrig}_i$  (scale on right axis) and  $\mathbf{XFP}_i$  (scale on the left axis) for the same sample paths.

The  $\mathbf{XFP}$  stays at the value (“has been stopped”) it took at the first time when it breached the barrier level as shown for the sample paths highlighted (in color online). If the barrier is never touched,

$\mathbf{XFP}$  is just  $X$ . The corresponding dashed lines,  $\mathbf{XTrig}$ , take the value 1.0 (true) at the time of barrier breach for the highlighted sample paths and otherwise stays at 0.0.

In the case with several barriers or more complicated barrier domains and conditions,  $\mathbf{tFP}_N$  and  $\mathbf{XFP}_N$  would identify the time and place the barrier was hit and thereby identify the barrier.

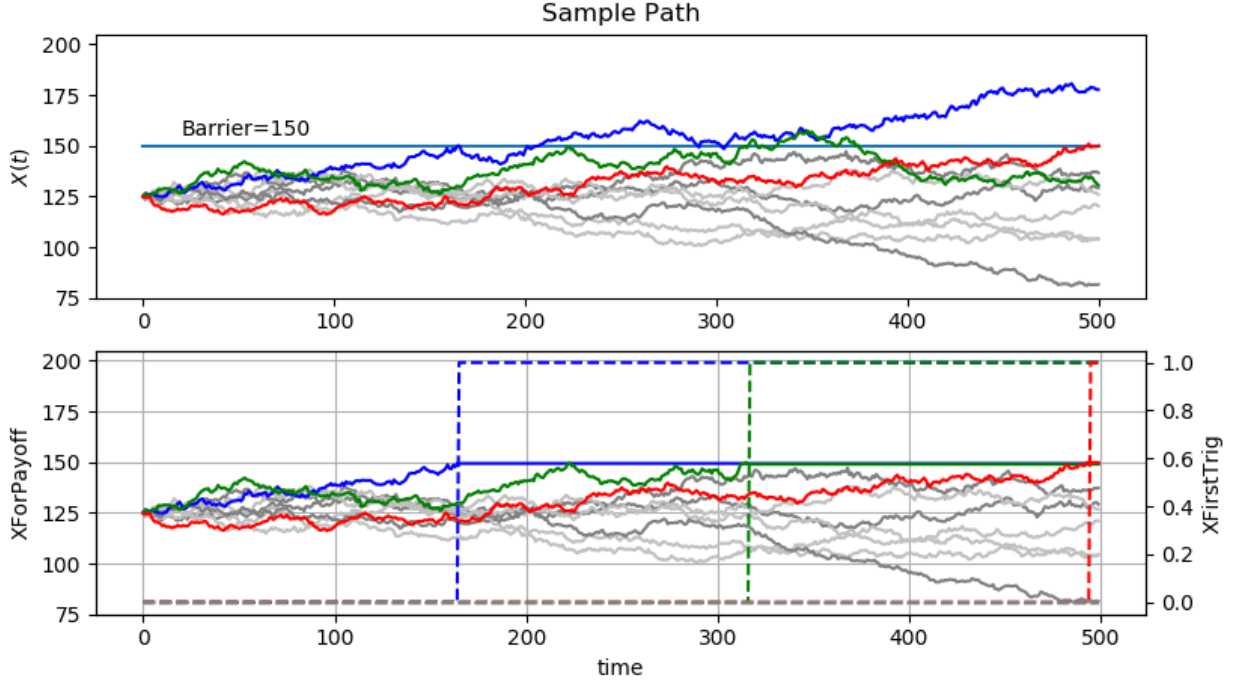


Figure 3: Behavior of conditional barrier triggers

## 6 Results

We perform testing in one and ten dimensions for Up-and-Out Calls on a single underlier or a geometric basket of underliers following Black-Scholes models.

For an one-dimensional Black-Scholes model with constant coefficients  $r$  and  $\sigma$ , the price of an Up-and-Out Call with maturity  $T$  at time  $t$  and  $S_t$  with time-to-maturity  $\tau = T - t$  can be computed as follows<sup>1</sup>:

<sup>1</sup>This is the result given, for instance, in chapter 11 of (Privault, 2021), written in a more compact form.

$$\delta_{\pm}^{\tau}(s) = \frac{1}{\sigma\sqrt{\tau}} \left( \log s + \left( r \pm \frac{\sigma^2}{2} \right) \tau \right) \quad (33)$$

$$F_{\pm}(s) = \Phi \left( \delta_{\pm}^{\tau} \left( \frac{B}{K} s \right) \right) - \Phi \left( \delta_{\pm}^{\tau}(s) \right) \quad (34)$$

$$G_{\pm}(s) = F_{\pm}(s) - \left( \frac{1}{s} \right)^{\pm 1 + \frac{2r}{\sigma^2}} F_{\pm} \left( \frac{1}{s} \right) \quad (35)$$

$$\text{OUC}(t, S_t) = 1_{M_0^t < B} \left( S_t G_+ \left( \frac{S_t}{B} \right) - e^{-\tau r} K G_- \left( \frac{S_t}{B} \right) \right) \quad (36)$$

with  $M_0^t = \sup_{s \in (0, t]} S_s$  being the minimum so far and  $\Phi$  being the cumulative density function of a standard normal.

Assuming that there are  $n$  correlated Black-Scholes models  $\frac{dS_i}{S_i} = \mu_i dt + \sigma_i dW_i$  with  $dW_i dW_j = \rho_{ij} dt$ , one can easily show that the geometric basket  $GB(t) = \prod_{i=1}^n S_i(t)^{\alpha_i}$  will follow  $\frac{dGB}{GB} = \bar{\mu} dt + \bar{\sigma} dW$  with

$$\bar{\sigma} = \sqrt{\sum_{i,j=1}^n \alpha_i \alpha_j \rho_{ij} \sigma_i \sigma_j} \quad \bar{\mu} = \frac{\bar{\sigma}^2}{2} + \sum_{i=1}^n \alpha_i \left( \mu_i - \frac{\sigma_i^2}{2} \right) \quad (37)$$

We thus can analytically price an Up-and-Out Call on a geometric basket in an arbitrary number of dimensions.

If barrier breach is only monitored at discrete, regular times (such as during MC simulation at regular intervals), (Kou, 2003) shows that the pricing impact of discrete observation can be approximated by shifting the barrier away from spot by a certain multiplicative barrier correction,  $e^{\beta \sigma \sqrt{\Delta T}}$  for  $\Delta T$  being the size of the time step,  $\beta = -\zeta(\frac{1}{2})/\sqrt{2\pi}$  with  $\zeta$  the Riemann zeta function, and then pricing a barrier option with continuous observation with that barrier level.

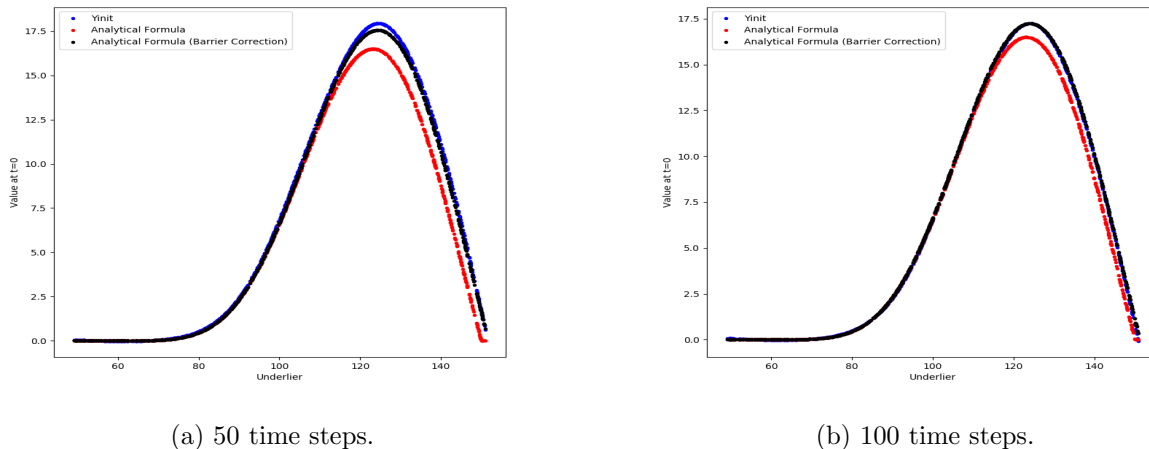
We use the parameters of the dynamics and instrument parameters as given in Table 2, along with initial value for the underliers chosen uniformly between 49 and 151. For the ten-dimensional case, we use ten uncorrelated such models for the components and we use the geometric mean of the underliers raised to 1.05 as a basket underlier. The final payoff and the barrier is defined in terms of that basket underlier. We note that Up-and-Out Calls without rebate have a discontinuous  $g_B$  function and are known to be challenging, especially close to the corner of discontinuity.

As for the FBSDE generator, we use the generator  $f(t, X_t, Y_t, Z_t) = -r(t, X_t)Y_t$  for the risk-neutral (discounting-only) case, as shown in section 2. However, any generator such as a generator for differential rates or other nonlinear pricing settings could be easily used instead.

We use softplus as a (differentiable) activation function. We train separate networks for the strategy function  $\pi_t$  at different times  $t$  and a separate network for the  $Y_0$  function. We tested several combinations of number of hidden layers and of neurons in each layer. More neurons on fewer layers performed better and so we used 20 neurons in 2 hidden layers for the one-dimensional case and 40 neurons in 2 hidden layers for the ten-dimensional case. Using more neurons than that in each layer

$\sigma$	$r$	$T$	$B$ (Barrier Position)	$K$ (Strike)
0.2	0.05	0.5 Years	150.0	100.0

Table 2: Parameters for the  $X$  dynamics, the generator, and the instruments



(a) 50 time steps.

(b) 100 time steps.

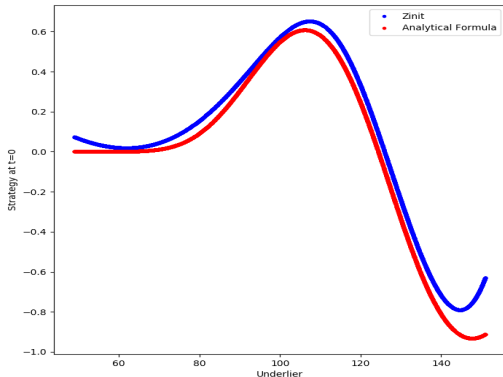
Figure 4: DeepBSDE value for one-dimensional Up-and-Out Call with different number of time steps (20 neurons in 2 hidden layers).

did not seem to improve results materially and neither did using more layers. We also tested a ResNet architecture as in (Cyr et al., 2019) and observed similar but not better results.<sup>2</sup>

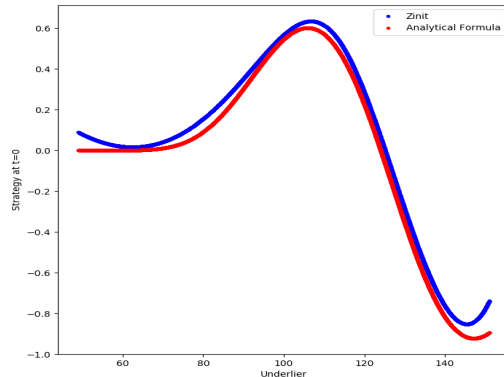
We used Adam optimizer based on mini-batch gradient descent with various mini-batch sizes and report results with mini-batches of size 1024. Larger mini-batch sizes lead to better approximation of the loss function. However, a mini-batch size of 1024 already leads to good visual approximation of the analytical solution in appropriate settings. We report 20,000 mini-batch steps but results for 10,000 mini-batches look similar. We use exponentially decaying learning rate, starting at 0.01 and decaying by 0.95 every 1,000 mini-batches. Running the forward pathwise DeepBSDE method for barriers takes similar time as the corresponding forward pathwise DeepBSDE method for instruments without barriers. We have not tried to aggressively optimize the learning rate schedule or other features of the methods. Even so, the results for ten-dimensional example are encouraging and we obtained good representations of solution and strategy. We will leave further performance improvements through different architectures or algorithmic choices to future work.

In Figures 4a and 4b we show the DeepBSDE solution  $Y_0(X_0)$  (denoted Yinit here and in following figures) for 50 and 100 time steps against the analytical solution with the original barrier position and the continuity corrected barrier position. While there are still visual differences to the continuity corrected analytical solution for 50 time steps, the solution for 100 time steps agrees visually with the analytical solution where the barrier position is corrected for the discrete monitoring of the barrier

<sup>2</sup>Note that (Cyr et al., 2019) considers approximation problems while here we solve stochastic control problems optimizing over an entire computational graph.



(a) 50 time steps.



(b) 100 time steps.

Figure 5: DeepBSDE strategy for one-dimensional Up-and-Out Call with different number of time steps, on ten mini-batches (20 neurons in 2 hidden layers).

in the simulation. We see that with increasing number of time steps, the continuity corrected and the original analytical solution get closer and the DeepBSDE solution approximates the continuity corrected analytical solution.

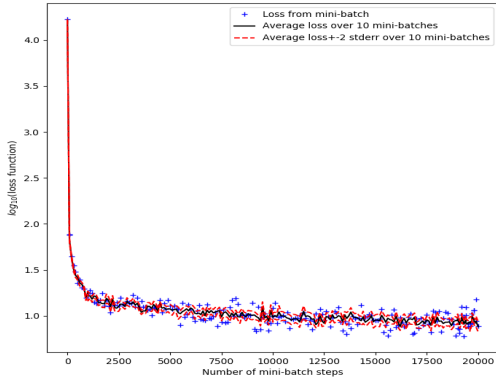
In Figures 5a and 5b, we compare the hedging strategy at time zero as determined by DeepBSDE (called  $\pi_0$  earlier in the paper and denoted Zinit in the Figure) and the analytical delta for the analytical solution with continuity corrected barrier position. We see that they generally agree in shape and are reasonably close. For small values of the underlier, the DeepBSDE strategy is not flat, but the strategy in that region does not have a strong impact on the loss function or on the value function.<sup>3</sup> For larger values of the underlier closer to the barrier, the DeepBSDE strategy is smaller in magnitude than the analytical strategy. Recall however that the analytical strategy assumes continuous hedging rather than discrete hedging and thus does not take into account that stock price might have entered and remained in the barrier during the time step before rehedging is possible. Looking at the later Figure 8b, we see that the P&L at barrier breach is skewed to negative P&L. All other things being equal, a less negative  $\pi_t$  will increase the P&L at barrier breach, make it more symmetric around 0, and reduce the value of the loss function, compared to using the more negative analytical delta close to the barrier.

Figures 6a and 6b show the evolution of the loss function during training for the cases with hedging at 50 and 100 time steps. Since we are training one network for each time step, more time steps mean more parameters to train so minima might be harder to find. More time steps also mean more frequent hedging and therefore a chance to reduce P&L more. In the one-dimensional case, one can see that more time steps allow DeepBSDE to find strategy with smaller mean square P&L (smaller loss function).

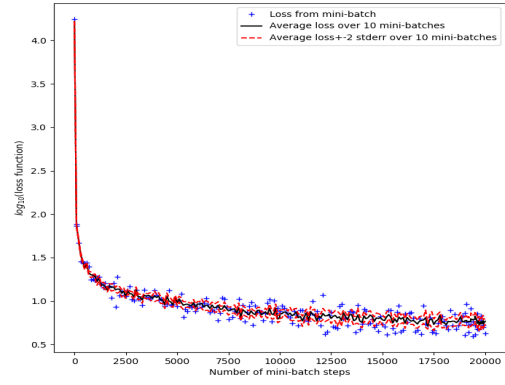
Figures 7a and 7b show how well the DeepBSDE strategy replicates that payoff at maturity and

<sup>3</sup>If correct asymptotics are required, one can embed such asymptotics in the network architecture for the strategy. We will leave such to future work.



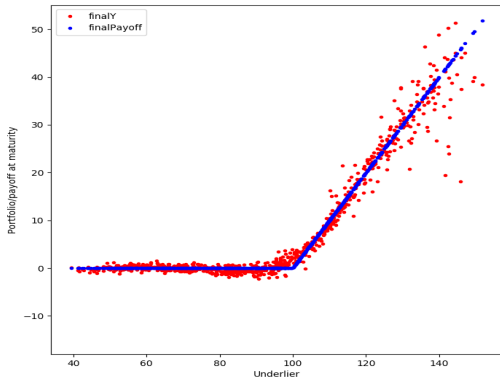


(a) 50 time steps.

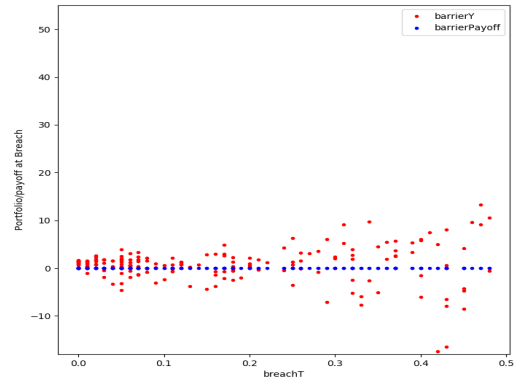


(b) 100 time steps.

Figure 6: DeepBSDE loss function over number of mini-batch steps for one-dimensional Up-and-Out Call with different number of time steps.

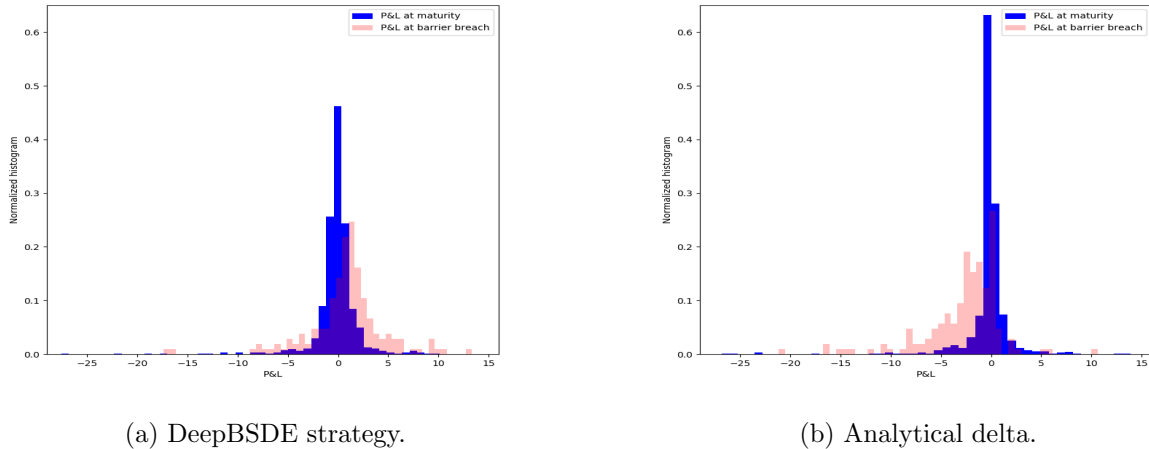


(a) At maturity.



(b) At barrier.

Figure 7: DeepBSDE: replication of maturity and barrier payoff. One-dimensional case, 50 time steps.



(a) DeepBSDE strategy.

(b) Analytical delta.

Figure 8: P&L from DeepBSDE method vs. analytical delta from continuous-time problem. One-dimensional case, 50 time steps.

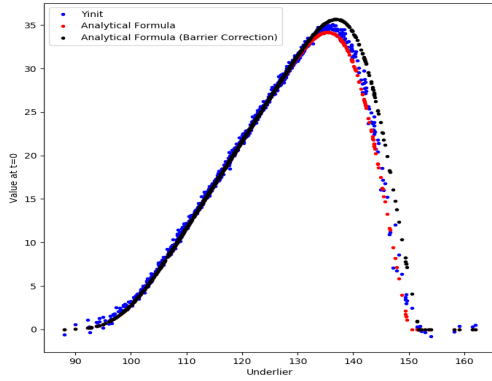
the knock-out barrier.

Figures 8a and 8b show histograms for the P&L for the strategy computed by DeepBSDE and the strategy given by the analytical delta of the analytical solution of the continuous problem with the same barrier. One can see that the final P&Ls span a similar range and the analytical strategy peaks a bit higher, but otherwise they have similar quantiles. The barrier P&L for the analytical strategy is asymmetric and mostly negative while the barrier P&L for the DeepBSDE strategy is more symmetric, leading to better P&L behavior at barrier breach.

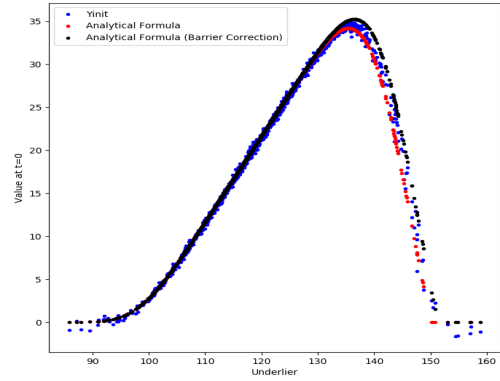
Figures 9a, 9b, 9c, and 9d show the DeepBSDE solution for the ten-dimensional example for different number of time steps. We are showing results both for a standard fully connected DNN for  $Y_0$  (top) and another architecture in which positive part is applied to the output of the DNN. We projected points in  $X$  space to the geometric basket underlier. Without being provided the geometric mean as a feature, the trained DNN gives very similar results for different  $X$  with the same geometric mean. The trained  $Y_0$  function approximates the analytical solution visually well. Close to the barrier, it is between the analytical solution without and with continuity correction. We are not aware of any other technique that would allow determining value function and strategy and hedging performance for high-dimensional barrier options. Figure 10a shows the evolution of the loss function during training for 100 time steps case, showing convergence similar to the one-dimensional case. Figure 10b shows that the final and barrier P&L histogram in ten dimensions looks similar to the one in one dimension, demonstrating that the DeepBSDE method works similarly well in low and high dimensions.

## 7 Conclusion

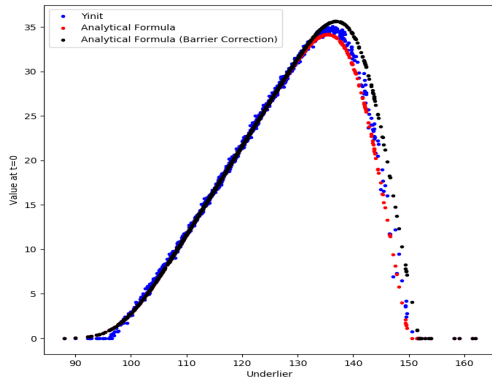
We proposed a novel deep neural network based computational graph architecture to price Barrier Options via DeepBSDE, that captures whether the underliers' price movement triggered the barrier or



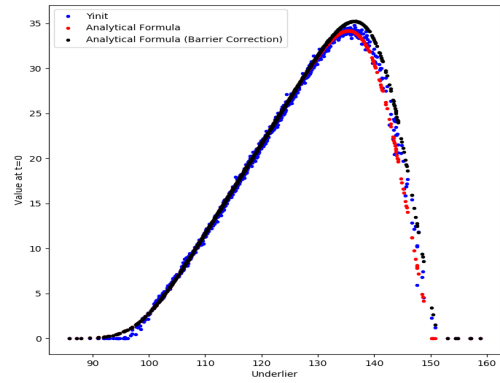
(a) 50 time steps.



(b) 100 time steps.

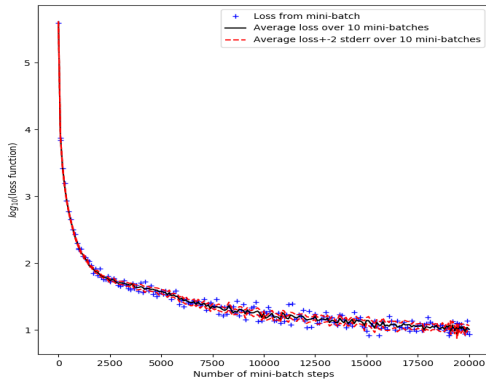


(c) 50 time steps, positive.

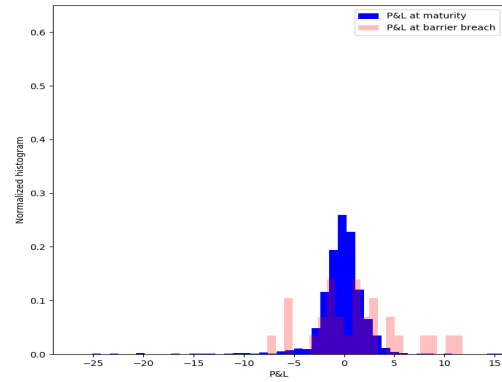


(d) 100 time steps, positive.

Figure 9: DeepBSDE value for ten-dimensional Up-and-Out Call on a geometric basket with different number of time steps (40 neurons in 2 hidden layers).



(a) Loss function.



(b) Final and barrier P&L.

Figure 10: DeepBSDE loss function and final and barrier P&L for ten-dimensional Up-and-Out Call with 100 time steps (40 neurons in 2 hidden layers).

not in order to model the appropriate payoff conditions and minimize the payoff error in order to learn the price of the option at initial time and the hedging strategy at hedging times. We also demonstrated the effectiveness of the hedging strategy via DeepBSDE learned Deltas at discrete time instances.

## 8 Acknowledgement

The authors would like to thank Fernando Cela Diaz and Pallavi Abhang for their help on setting up and running on distributed computing infrastructure, Orcan Ogetbil for discussions on barrier option pricing, Vijayan Nair for discussion regarding methods, presentation, and results and Agus Sudjianto for supporting this research. The authors also would like to thank the two anonymous reviewers and the editors for their comments that substantially improved the quality of the paper. The authors report no conflicts of interest. The authors alone are responsible for the content and writing of the paper.

## References

- Chan-Wai-Nam, Q., Mikael, J., and Warin, X. (2019). Machine learning for semi linear PDEs. *Journal of Scientific Computing* 79(3), 1667–1712. arXiv:1809.07609.
- Cyr, E. C., Gulian, M. A., Patel, R. G., Perego, M., and Trask, N. A. (2019). Robust training and initialization of deep neural networks: An adaptive basis viewpoint. *arXiv preprint arXiv:1912.04862*.
- El Karoui, N., Peng, S., and Quenez, M. C. (1997). Backward stochastic differential equations in finance. *Mathematical finance* 7(1), 1–71. Also available on semanticscholar.org.
- Han, J., Jentzen, A., and E, W. (2018). Solving high-dimensional partial differential equations using deep learning. *Proceedings of the National Academy of Sciences* 115(34), 8505–8510.

- Hientzsch, B. (2019). Introduction to solving quant finance problems with time-stepped FBSDE and deep learning. *arXiv preprint arXiv:1911.12231*. Also available at SSRN: <https://ssrn.com/abstract=3494359> or <http://dx.doi.org/10.2139/ssrn.3494359>.
- Kou, S. (2003). On pricing of discrete barrier options. *Statistica Sinica* 13, 955–964.
- Kremsner, S., Steinicke, A., and Szölgényi, M. (2020). A deep neural network algorithm for semilinear elliptic PDEs with applications in insurance mathematics. *arXiv preprint arXiv:2010.15757v2*.
- Lejay, A. (2002). BSDE driven by dirichlet process and semi-linear parabolic PDE. Application to homogenization. *Stochastic processes and their applications* 97(1), 1–39.
- Mercurio, F. (2015). Bergman, Piterbarg, and beyond: Pricing derivatives under collateralization and differential rates. In *Actuarial Sciences and Quantitative Finance*, pp. 65–95. Springer. Also available at SSRN: <https://ssrn.com/abstract=2326581> or <http://dx.doi.org/10.2139/ssrn.2326581>.
- Pardoux, É. (1998). Backward stochastic differential equations and viscosity solutions of systems of semilinear parabolic and elliptic PDEs of second order. In *Stochastic Analysis and Related Topics VI*, pp. 79–127. Springer.
- Perkowski, N. (2010). Backward Stochastic Differential Equations: An introduction. Available on [semanticscholar.org](https://www.semanticscholar.org).
- Privault, N. (2021). Notes on stochastic finance. Lecture Notes. Available at <https://www.ntu.edu.sg/home/nprivault/index.html>.
- Raissi, M. (2018). Forward-backward stochastic neural networks: Deep learning of high-dimensional partial differential equations. *arXiv preprint arXiv:1804.07010*.
- Shreve, S. (2004). *Stochastic Calculus for Finance II*. Springer-Verlag New York.
- Yu, B., Xing, X., and Sudjianto, A. (2019). Deep-learning based numerical BSDE method for Barrier options. *arXiv preprint arXiv:1904.05921*. Also available at SSRN: <https://ssrn.com/abstract=3366314> or <http://dx.doi.org/10.2139/ssrn.3366314>.